doi:10.1246/cl.2010.1251
Published on the web October 30, 2010

Lignin Gasification over Charcoal-supported Palladium and Nickel Bimetal Catalysts in Supercritical Water

Aritomo Yamaguchi,[1] Norihito Hiyoshi,[1] Osamu Sato,[1] Mitsumasa Osada,[2] and Masayuki Shirai*[1]
[1]*Research Center for Compact Chemical System, National Institute of Advanced Industrial Science and Technology (AIST), 4-2-1 Nigatake, Miyagino-ku, Sendai, Miyagi 983-8551*
[2]*Department of Chemical Engineering, Ichinoseki National College of Technology, Takanashi, Hagisho, Ichinoseki, Iwate 021-8511*

(Received September 13, 2010; CL-100786; E-mail: m.shirai@aist.go.jp)

Charcoal-supported palladium and nickel binary salt catalysts showed higher lignin gasification activity than the linear combination activities of the individual monometal catalysts, indicating a bimetallic synergetic effect. XRD and EXAFS analyses revealed that Pd–Ni alloy structures were formed during the lignin gasification over the catalysts, which provided higher activities for the gasification than the individual monometal catalysts.

Palladium and nickel form solid solution alloy over the entire composition,[1,2] and palladium–nickel (Pd–Ni) alloy catalysts have attracted attention because of synergetic effects of Pd–Ni on catalytic activities for some reactions, such as hydrogenation of nitrobenzene,[3] methane oxidative reforming,[4] and methanol oxidation.[1]

Supercritical water ($T_c = 647.3$ K, $P_c = 22.1$ MPa) gasification of lignin is a promising technique because of a decrease of lignin gasification temperature.[5,6] We have reported that charcoal-supported ruthenium(III) salts are reduced to form highly dispersed ruthenium metal particles during the lignin gasification, which are active for lignin gasification.[6] We applied palladium and nickel salts to gasification in order to prepare highly dispersed Pd–Ni alloy particles on charcoal support during the reaction and to investigate activity of Pd–Ni alloy, compared with the individual monometals.

The catalysts used in this work were prepared by impregnation using activated charcoal powder and aqueous solutions of tetraamminepalladium(II) nitrate or nickel(II) nitrate. The aqueous solution of metal precursor and charcoal powder were stirred for 1 h at ambient temperature and evaporated to dryness at 323 K under reduced pressure. Then the samples were dried for 10 h at 373 K in an oven (denoted as Pd(II)/C and Ni(II)/C). The amount of metal species in all the catalysts was regulated to be 5 wt %. Supported metal salt catalysts were used for lignin gasification in supercritical water. Reduced catalysts were also prepared by pretreatment in flowing hydrogen at 673 K for 2 h as reference (denoted as [Pd]red/C and [Ni]red/C). The supported binary metal salt catalysts were prepared by physically mixing two kinds of supported monometal salt catalysts (denoted as Pd(II)–Ni(II)/C).

Gasification of lignin was carried out in a batch reactor.[6] The lignin, catalyst, and water were loaded into a reactor, and the reactor was kept at 673 K for a given reaction time. After the reaction, gaseous products were analyzed by a gas chromatography. Liquid and solid products were separated into water-soluble, tetrahydrofuran (THF)-soluble, and THF-insoluble fraction. Product yield (C%) was calculated based on the carbon amount of reactant lignin, and gas composition (%) is defined as the moles of gas product divided by the sum of moles of gas products. The lignin gasification was conducted three times at each condition and the product yields were averaged.

X-ray absorption near edge structure (XANES) and extended X-ray absorption fine structure (EXAFS) measurements were performed using a synchrotron radiation ring in transmission mode at AR-NW10A, PF-KEK with a Si(311) double-crystal monochrometer for Pd K-edge and at BL-9C, PF-KEK with a Si(111) double-crystal monochrometer for Ni K-edge. The EXAFS spectra were analyzed by the UWXAFS package.[7] The backscattering amplitudes and phase shifts were calculated by the FEFF8 code.[8]

Table 1 shows the product yield of lignin gasification in supercritical water over supported monometal salt catalysts at 673 K for 1 h and reduced metal catalysts. The gas yields over the palladium and nickel catalysts were 12–18 C%, which were higher than the gas yield (8.4 C%) over charcoal without metal species, indicating that the palladium and nickel catalysts were active for lignin gasification. The palladium and nickel catalysts were not as active as the ruthenium catalysts; however it is notable that the selectivities of hydrogen (15%) and carbon monoxide (7–10%) over the supported palladium catalysts were high, compared with those over the other metal catalysts (hydrogen 3–6% and carbon monoxide 0–1%).[6] The supported metal salt catalysts Pd(II)/C and Ni(II)/C showed higher activities than the corresponding reduced metal catalysts. We confirmed that the palladium species in Pd(II)/C were completely reduced during the lignin gasification and that the palladium metal particles were formed from XANES and XRD; on the other hand, the nickel species were composed of zero (metal) and divalent nickel after lignin gasification for 1 h from XANES analysis and partially dissolved in water (Ni^{2+} species: 13% in [Ni]red/C and 6.2% of Ni(II)/C) from ICP analysis.

We carried out the lignin gasification in supercritical water using the mixture of Pd(II)/C and Ni(II)/C catalysts (Figure 1)

Table 1. Product yield and composition of catalytic lignin gasification in supercritical water (lignin 0.10 g, catalyst 0.15 g, water density 0.50 g cm^{-3}, 673 K, 1 h)

Catalyst	Product yield/C%			
	Gas	Water soluble	THF soluble	THF insoluble
[Pd]red/C	15 ± 1	8.8 ± 0.5	42 ± 2	34 ± 2
Pd(II)/C	18 ± 1	8.2 ± 0.5	48 ± 2	26 ± 1
[Ni]red/C	12 ± 1	9.1 ± 0.5	28 ± 1	51 ± 2
Ni(II)/C	14 ± 1	8.8 ± 0.5	52 ± 2	25 ± 1

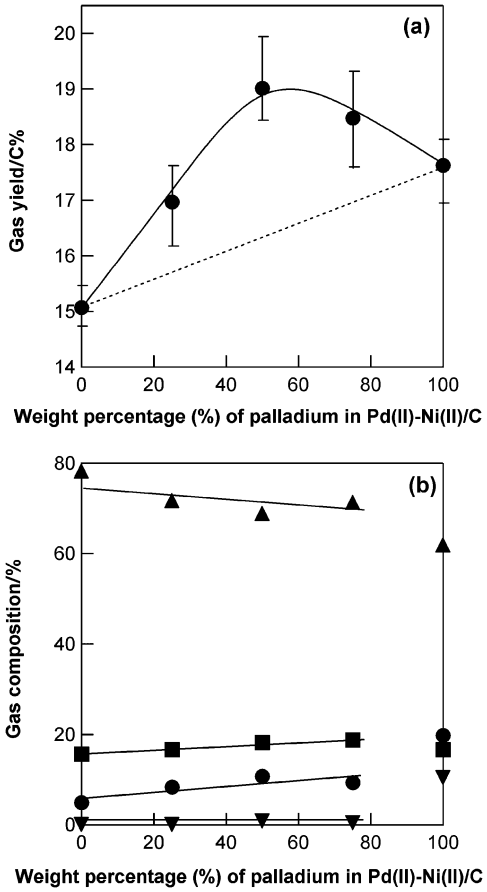

Figure 1. Gas yield (a) and gas composition (b) of catalytic lignin gasification in supercritical water at 673 K for 1 h over Ni(II)/C, Pd(II)–Ni(II)/C, and Pd(II)/C (H_2 (●), CH_4 (■), CO (▼), and CO_2 (▲)). The bars in (a) indicate ranges of the gas yields, which were measured three times at each condition.

as binary salt catalysts (Pd(II)–Ni(II)/C). The gas yields from the lignin gasification over the Pd(II)–Ni(II)/C catalysts were higher than the linear combination of gas yields over the individual monometals (Figure 1a), indicating that the Pd(II)–Ni(II)/C binary salt catalysts showed the synergetic effect of Pd–Ni. The selectivity of hydrogen and carbon monoxide over the monometal Pd(II)/C catalysts was high compared with that over the bimetal catalysts of Pd(II)–Ni(II)/C (Figure 1b). We investigated the structure of the Pd(II)–Ni(II)/C catalysts to understand the synergetic effect of Pd–Ni on the catalytic activity. Figure 2 shows XRD patterns of the Pd(II)–Ni(II)/C catalysts (weight ratio; 3:1, 1:1, and 1:3, denoted as Pd(II)–Ni(II)/C(3:1), Pd(II)–Ni(II)/C(1:1), and Pd(II)–Ni(II)/C(1:3)) after lignin gasification in supercritical water at 673 K for 1 h. The XRD peaks at 40.0 and 46.5 degrees attributed to palladium metal (JCPDS 88-2335) were observed in the Pd(II)/C after the reaction. On the other hand, the XRD peaks attributed to nickel metal (44.3 and 51.6 degrees, JCPDS 89-7128) and nickel oxide (NiO, 37.2 and 43.3 degrees, JCPDS 44-1159) were observed in the Ni(II)/C catalyst after the gasification. The catalysts were dried after the reaction, followed by XRD measurement under ex situ conditions. The Ni metal particles in the Ni(II)/C catalyst would be oxidized by air before XRD analysis, resulting in the

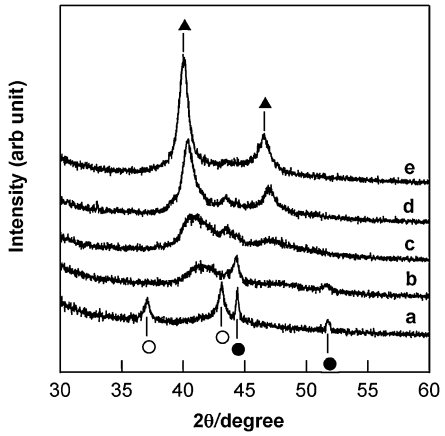

Figure 2. XRD patterns for Ni(II)/C, Pd(II)–Ni(II)/C, and Pd(II)/C catalysts after lignin gasification in supercritical water at 673 K for 1 h (catalyst: (a) Ni(II)/C, (b) Pd(II)–Ni(II)/C(1:3), (c) Pd(II)–Ni(II)/C(1:1), (d) Pd(II)–Ni(II)/C(3:1), and (e) Pd(II)/C). The closed circles, open circles, and closed triangles indicate nickel metal, nickel oxide, and palladium metal.

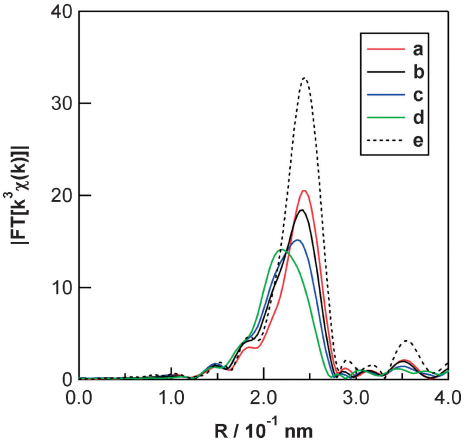

Figure 3. Fourier transforms of k^3-weighted Pd K-edge EXAFS spectra of Pd(II)–Ni(II)/C and Pd(II)/C catalysts after lignin gasification in supercritical water at 673 K for 1 h (phase shift uncorrected). Catalyst: (a) Pd(II)/C, (b) Pd(II)–Ni(II)/C(3:1), (c) Pd(II)–Ni(II)/C(1:1), (d) Pd(II)–Ni(II)/C(1:3), and (e) reference Pd metal foil.

formation of NiO particles. The XRD patterns of the Pd(II)–Ni(II)/C catalysts are different from those of the monometal catalysts (Figure 2), indicating that the structures of metal particles in Pd(II)–Ni(II)/C catalysts are different from a physical mixture of the correspond monometal particles and should have Pd–Ni alloy structures.

Fourier transforms of k^3-weighted EXAFS (FT-EXAFS) spectra at the Pd K-edge of the Pd(II)–Ni(II)/C bimetal catalysts after lignin gasification in supercritical water at 673 K for 1 h were compared with that of Pd(II)/C (Figure 3). In the case of Pd(II)/C, the main peak is attributed to a Pd–Pd metal bond. The main peaks for Pd(II)–Ni(II)/C(3:1), Pd(II)–Ni(II)/C(1:1), and Pd(II)–Ni(II)/C(1:3) gradually decrease and shift to a shorter distance with the decrease of Pd/Ni ratio, indicating the formation of a Pd–Ni bond in addition to a Pd–Pd bond. The

peak shift of both XRD patterns (Figure 2) and the FT-EXAFS spectra (Figure 3) showed that the Pd(II)–Ni(II)/C bimetal catalysts had alloy structures. It is well known that nickel and palladium form complete solid solutions in the case of bulk metals.[9] The XRD and FT-EXAFS indicate that the Pd(II)–Ni(II)/C bimetal catalysts have bimetal particles with solid solution alloy. The higher gas yields of the lignin gasification over the Pd(II)–Ni(II)/C bimetal catalysts may be caused by the Pd–Ni alloy structures. ICP analysis revealed that palladium species were not dissolved in water from the Pd(II)–Ni(II)/C catalysts after the gasification; however, 7.3, 6.0, and 16.8% of nickel in Pd(II)–Ni(II)/C(3:1), Pd(II)–Ni(II)/C(1:1), and Pd(II)–Ni(II)/C(1:3) were dissolved in water after the lignin gasification (673 K, 1 h), respectively, indicating that nickel species in the Pd(II)–Ni(II)/C catalysts were not reduced completely.

We also investigated the catalytic activities and the structure of the prereduced Pd–Ni bimetal catalysts in hydrogen (H_2) at 673 K. We prepared three kinds of Pd–Ni bimetal catalysts pretreated in H_2; (1) charcoal powder was impregnated with solution of $Pd(NH_3)_4(NO_3)_2$ and $Ni(NO_3)_2$, followed by pretreatment in H_2 at 673 K for 2 h (denoted as [Pd–Ni]red/C), (2) Pd(II)/C was treated in H_2 at 673 K for 2 h, followed by impregnation with $Ni(NO_3)_2$ solution (denoted as [Pd]red–Ni(II)/C), and (3) Ni(II)/C was treated in H_2 at 673 K for 2 h, followed by impregnation with $Pd(NH_3)_4(NO_3)_2$ solution (denoted as [Ni]red–Pd(II)/C). The order of activity for the lignin gasification among the Pd–Ni bimetal catalysts in terms of gas yield (Table 2) was the following: Pd(II)–Ni(II)/C > [Pd–Ni]red/C ≈ [Ni]red–Pd(II)/C ≫ [Pd]red–Ni(II)/C. The Pd(II)–Ni(II)/C, [Pd–Ni]red/C, and [Ni]red–Pd(II)/C catalysts showed higher gas yields than those over the individual monometal catalysts, indicating that the synergetic effect of Pd–Ni was observed in those catalysts; however, the synergetic effect of Pd–Ni was not observed in the [Pd]red–Ni(II)/C catalyst. Pd K-edge FT-EXAFS spectra of the prereduced Pd–Ni bimetal catalysts after lignin gasification were measured (Figure S1 in Supporting Information[10]) to investigate bimetal structures. The peak shift of FT-EXAFS, which was attributed to Pd–Ni bond formation, was observed for the Pd(II)–Ni(II)/C, [Pd–Ni]red/C, and [Ni]red–Pd(II)/C catalysts, indicating formation of the Pd–Ni alloy. On the other hand, the FT-EXAFS peak shift was not observed for [Pd]red–Ni(II)/C, indicating that the Pd–Ni alloy was not formed. The palladium and nickel species in Pd(II)–Ni(II)/C and [Pd–Ni]red/C catalysts were reduced at the same time during the lignin gasification or H_2 treatment, resulting in the formation of Pd–Ni alloy structures. In the case of [Ni]red–Pd(II)/C, nickel metal species were partially dissolved in water during the lignin gasification, which were confirmed by ICP analysis, and the dissolved nickel species and $Pd(NH_3)_4(NO_3)_2$ species were reduced during the lignin gasification, forming the Pd–Ni alloy structures. Palladium metal particles, however, were not dissolved in water during the lignin gasification; therefore, the Pd–Ni alloy structures were not formed on the [Pd]red–Ni(II)/C catalyst. The synergy of palladium and nickel was observed over the catalysts having Pd–Ni alloy structures. We observed smaller metal particles in Pd(II)–Ni(II)/C (50 nm) than [Pd–Ni]red/C (100–200 nm) and [Ni]red–Pd(II)/C (100–200 nm) by TEM measurements. The palladium and nickel species in Pd(II)–Ni(II)/C were reduced to small Pd–Ni alloy particle during the lignin gasification. We conclude that divalent palladium and nickel salts were reduced during the lignin gasification to form small Pd–Ni alloy particles, which provide higher activities for the lignin gasification than the linear combination of individual monometals.

Table 2. Product yield of catalytic lignin gasification in supercritical water (lignin 0.10 g, catalyst 0.15 g, water density 0.50 g cm^{-3}, 673 K, 1 h, weight ratio of Pd/Ni is 1.0 for all catalysts)

Catalyst	Product yield/C%			
	Gas	Water soluble	THF soluble	THF insoluble
Pd(II)–Ni(II)/C	19 ± 1	9.7 ± 0.5	44 ± 2	26 ± 1
[Pd–Ni]red/C	18 ± 1	13 ± 1	38 ± 2	31 ± 2
[Pd]red–Ni(II)/C	15 ± 1	8.6 ± 0.5	39 ± 2	37 ± 2
[Ni]red–Pd(II)/C	18 ± 1	11 ± 1	40 ± 2	31 ± 2

EXAFS measurements were done with the approval of the PAC committee (proposal No. 2009G001). This work has been supported by Special Coordination Funds for Promoting Science and Technology of Ministry of Education, Culture, Sports, Science and Technology (MEXT), Japan.

References and Notes

1 T. Shobha, C. L. Aravinda, P. Bera, L. G. Devi, S. M. Mayanna, *Mater. Chem. Phys.* **2003**, *80*, 656.
2 P. V. Petrenko, A. V. Gavrilyuk, N. P. Kulish, N. A. Melnikova, Y. E. Grabovskii, *Phys. Met. Metallogr.* **2009**, *108*, 449.
3 N. Toshima, P. Lu, *Chem. Lett.* **1996**, 729; P. Lu, T. Teranishi, K. Asakura, M. Miyake, N. Toshima, *J. Phys. Chem. B* **1999**, *103*, 9673.
4 M. Nurunnabi, S. Kado, K. Suzuki, K. Fujimoto, K. Kunimori, K. Tomishige, *Catal. Commun.* **2006**, *7*, 488.
5 M. Osada, O. Sato, K. Arai, M. Shirai, *Energy Fuels* **2006**, *20*, 2337; M. Osada, O. Sato, M. Watanabe, K. Arai, M. Shirai, *Energy Fuels* **2006**, *20*, 930; M. Osada, T. Sato, M. Watanabe, M. Shirai, K. Arai, *Combust. Sci. Technol.* **2006**, *178*, 537; M. Osada, N. Hiyoshi, O. Sato, K. Arai, M. Shirai, *Energy Fuels* **2007**, *21*, 1400; M. Osada, N. Hiyoshi, O. Sato, K. Arai, M. Shirai, *Energy Fuels* **2007**, *21*, 1854; A. Yamaguchi, N. Hiyoshi, O. Sato, K. K. Bando, M. Osada, M. Shirai, *Catal. Today* **2009**, *146*, 192.
6 A. Yamaguchi, N. Hiyoshi, O. Sato, M. Osada, M. Shirai, *Energy Fuels* **2008**, *22*, 1485; A. Yamaguchi, N. Hiyoshi, O. Sato, M. Osada, M. Shirai, *Catal. Lett.* **2008**, *122*, 188.
7 E. A. Stern, M. Newville, B. Ravel, Y. Yacoby, D. Haskel, *Physica B* **1995**, *208–209*, 117.
8 A. L. Ankudinov, B. Ravel, J. J. Rehr, S. D. Conradson, *Phys. Rev. B* **1998**, *58*, 7565.
9 W. B. Pearson, *A Handbook of Lattice Spacings and Structures of Metals and Alloys*, Pergamon Press, New York, **1967**, Vols. 1 and 2.
10 Supporting Information is available electronically on the CSJ-Journal Web site, http://www.csj.jp/journals/chem-lett/index.html.

